ISSN: 0128-7680
Pertanika J. Sci. & Technol. **17 (2)**: 219 – 230 (2009)

Modelling of Precast Concrete Composite Slab Using Finite and Interface Elements

M.S. Jaafar, J.N. Wong, J. Noorzaei* and W.A. Thanoon
Department of Civil Engineering, Faculty of Engineering,
Universiti Putra Malaysia, 43400 UPM, Serdang, Selangor, Malaysia
**E-mail: jamal@eng.upm.edu.my*

ABSTRACT

This study presents an efficient finite element analysis technique which shows great versatility in modelling of precast composite flooring system subjected to static loadings. The method incorporates sliding and opening in the analysis of composite structures using the interface element which was specifically designed to simulate the actual behaviour at the interfaces between contacting materials. A three-dimensional finite element model of the precast composite slab which exhibits discontinuous behaviour was performed to demonstrate the potential and applicability of the proposed method of analysis. The results of the analysis demonstrate that the overall response of a discontinuous system to external loading is significantly affected by the bonding condition at the interfaces between the contacting materials.

Keywords: Finite element method, interface, isoparametric, composite, precast

INTRODUCTION

The viability of the finite element method, for the analysis and design of composite structures, has been proven by several researchers. For example, Tzamtzis *et al*. (2004a, b) model the interfacial behaviour between the brick and mortar, in case of masonry walls, under static and dynamic loadings. Different imperfect transmission conditions which model a thin intermediate layer, between two bonded materials with dissimilar material properties, were carried out by Mishuris *et al*. (2005) using interface element. Meanwhile, three-dimensional simulation of the crack in beams was carried out by Hanson *et al*. (2003) using interface element. The steel-concrete composite plate girders, under the action of shear and bending, were investigated by Baskar *et al*. (2003) using shell and interface elements through ABAQUS commercial software. A similar work was also reported by Nassif *et al*. (2004).

This investigation presents a computational model used for the discretisation of the composite flooring/roofing system. The slab unit is composed of precast and *in situ* concrete.

FORMULATION OF THE JOINT ELEMENT

Proposed finite element modelling:
The precast composite slabs are constructed into two layers, namely the precast and *in situ* layers. Each layer has different material properties.

Received: 6 July 2007
Accepted: 19 January 2009
*Corresponding Author

The following elements were used to discretize the precast composite slab:

i. Sixteen noded three-dimensional isoparametric finite elements to model the top and bottom layers
ii. Sixteen noded isoparametric interface element

Hence, this study was carried out to model each layer separately and to account for the interfacial behaviour between the layers, in which a special joint/interface element (sandwiched between the two sixteen noded isoparametric brick elements shown in *Fig. 1a*) was formulated. A brief formulation of this element (*Fig. 1*) is presented in the following discussion.

$$X = \sum_{i=1}^{n} N_i X_i;\ Y = \sum_{i=1}^{n} N_i Y_i;\ Z = \sum_{i=1}^{n} N_i Z_i \tag{1}$$

For corner nodes:

$$N_i = \frac{1}{4}(1 + \xi\xi_i)(1 + \zeta\zeta_i)(\xi\xi_i + \zeta\zeta_i - 1);\ i = \text{I, III, V and VII} \tag{2}$$

For midside nodes:

(a) $\xi = 0.0$

$$N_i = \frac{1}{2}(1 + \zeta\zeta_i)(1 - \xi^2);\ i = \text{II and VI} \tag{3}$$

(b) $\zeta = 0.0$–

$$N_i = \frac{1}{2}(1 + \xi\xi_i)(1 - \zeta^2);\ i = \text{IV and VIII} \tag{4}$$

$$U = \sum_{i=1}^{n} N_i U_i;\ V = \sum_{i=1}^{n} N_i V_i;\ W = \sum_{i=1}^{n} N_i W_i \tag{5}$$

where X, Y, Z and ξ, η, ζ are global and natural coordinate systems, respectively.

U, V and W are the displacement components with respect to global coordinate system.

n is the number of nodes.

N_i are the shape functions.

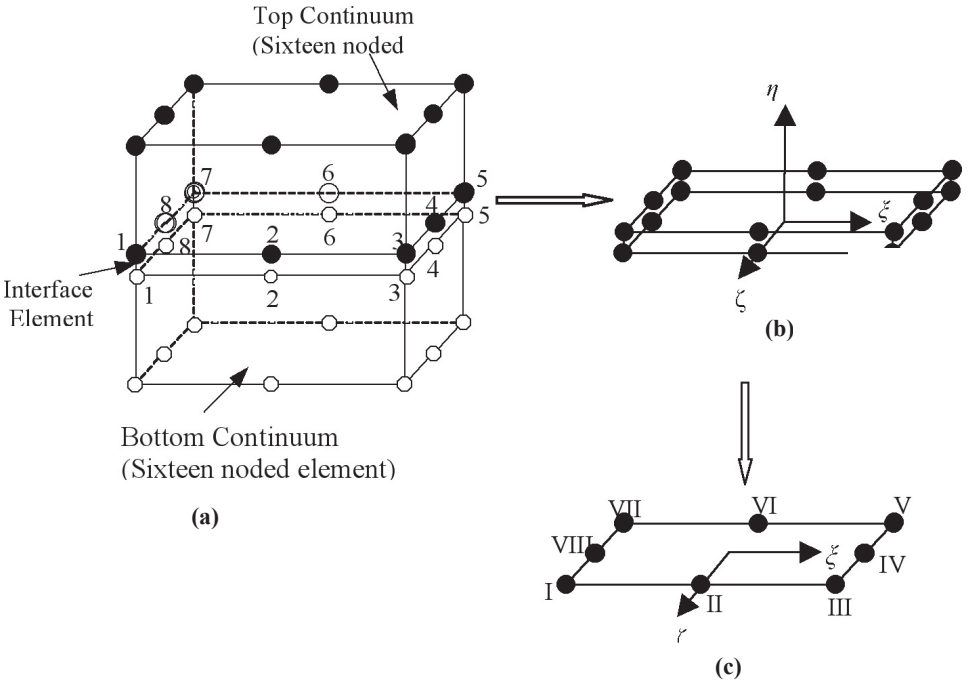

Fig. 1: Interface elements sandwiched between two horizontal layers

The interface nodes of the top and bottom continuum possess the same coordinates, that is zero thickness, and their relative displacements are given by:

$$\{\Delta\}=[I,-I]\{\delta\} \tag{6}$$

where $[I]$ = Identity matrix

Defining $[T] = [I, -I]$, so this can written as follows:

$$\{\Delta\} = [T]_{16*48} \quad \{\delta\}_{48*1} \tag{7}$$

Here, $\{\Delta\}$ is defined as:

$$\{\Delta U_1, \Delta V_1, \Delta W_1, ..., \Delta U_{VIII}, \Delta V_{VIII}, \Delta W_{VIII}\} \tag{8}$$

The present interface element, formulated for the use at the interface between two sixteen node isoparametric brick element (in ξ-ζ plane), and the typical parabolic interface element is shown in *Fig. 1b*. The pairs of 1-1, 2-2, …., 8-8 are usually close to each other.

$$\Delta U_I = U_2^t - U_2^b;\ \Delta V_I = V_2^t - V_2^b;\ \Delta W_I = W_2^t - W_2^b \tag{9}$$

Suffixes *t* and *b* denote the top and bottom continuum. Similar expression can be written for the other relative displacement, i.e. for node II, III, IV, ……, VIII. In the case of the interface element, the strains can be expressed as:

$$\{\varepsilon\} = \{\Delta U, \Delta V, \Delta W\} \tag{10}$$

$$\text{where } \Delta U = \Delta U = \sum_{i=1}^{n} N_i \Delta U_i;\ \Delta V = \sum_{i=1}^{n} N_i \Delta V_i\ ;\ \Delta W = \sum_{i=1}^{n} N_i \Delta W_i \tag{11}$$

i = I, II, III, IV, V, VI, VII and VIII

$$\begin{Bmatrix} \Delta U \\ \Delta V \\ \Delta W \end{Bmatrix} = \begin{Bmatrix} N_I & 0 & 0 & N_{II} & 0 & 0 & \cdots\cdots \\ 0 & N_I & 0 & 0 & N_{II} & 0 & \cdots\cdots \\ 0 & 0 & N_I & 0 & 0 & N_{II} & \cdots\cdots \end{Bmatrix}_{3*48} \{\Delta\}_{48*1} \tag{12}$$

i.e. $\{\varepsilon\} = [N]\{\Delta\}$ (13)

Using Eq. (7),

$$\begin{aligned} \{\varepsilon\} &= [N]_{3*16}[T]_{16*48}\{\delta\}_{48*1} \\ &= [B_J]_{3*48}\{\delta\}_{48*1} \end{aligned} \tag{14}$$

where $[B_J]$ = Shape function matrix for joint element.

The stress-strain relation is expressed as in standard form:

$$\{\sigma\} = [D]\{\varepsilon\} \tag{15}$$

In the case of interface element, elasticity matrix is presented as:

$$[D] = \begin{bmatrix} K_{nn} & 0 & 0 \\ 0 & K_{ss} & 0 \\ 0 & 0 & K_{ss} \end{bmatrix}_{3*3} \tag{16}$$

where K_{nn} and K_{ss} are the normal and shear stiffness, respectively.

The stiffness matrix for joint element is given by:

$$[K] = \int_v [B_J]^T [D][B_J] dv \tag{17}$$

DEVELOPMENT OF FINITE ELEMENT CODE

The finite element code, which was written by Noorzaei *et al*. (2003), was further modified by including the 16-noded joint element which modelled the contact/interfacial behaviour between the two 16-noded isoparametric brick elements, two 20-noded or one 16-noded and one 20-noded isoparametric brick elements. The program runs under a master MAIN. The overall flowchart of this finite element code is presented in *Fig. 2*.

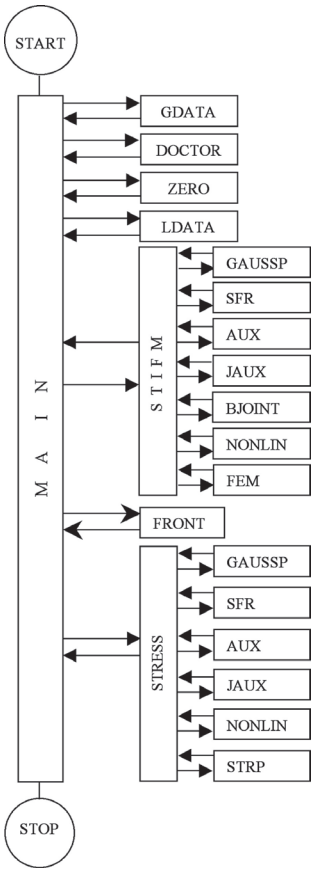

Fig. 2: Flow chart 3-D finite element code

PROBLEM ANALYSED

The plan view of the precast composite flooring system, together with the material properties for the precast layer and *in situ* layer, is shown in *Fig. 3*.

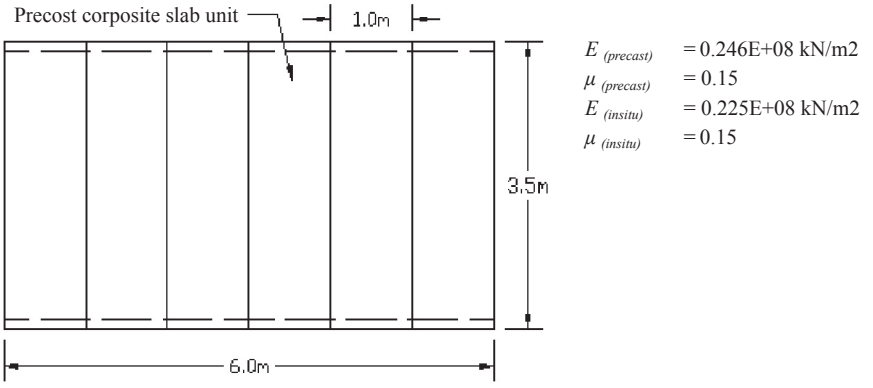

Fig. 3: Plan view of the precast composite flooring system

Only one unit of the precast composite slab was taken for the finite element analysis. For a single composite slab unit, the thickness of the precast layer is 75 mm and the cast *in situ* layer is 75 mm. As for the realistic finite element modelling of the composite slab unit, the interface element was used to account for the frictional behaviour between the two different layers of the composite slab modelled using 16-noded isoparametric brick element. *Fig. 4* shows the finite element mesh of the composite slab, with and without the interface elements.

In order to account for the composite action between the two layers, this example was analysed for different cases as presented in Table 1. Based on the investigation carried out by Pande *et al*. (1979) and Viladkar (1994), it was suggested that for full bond case $K_{ss} = K_{nn} = 10^6$-10^9 kN/m^2 could be assumed in absence of the experiment data. Meanwhile, for the no bond case, $K_{nn} = 10^6$-10^9 kN/m^2 and $K_{ss} = 0.0$.

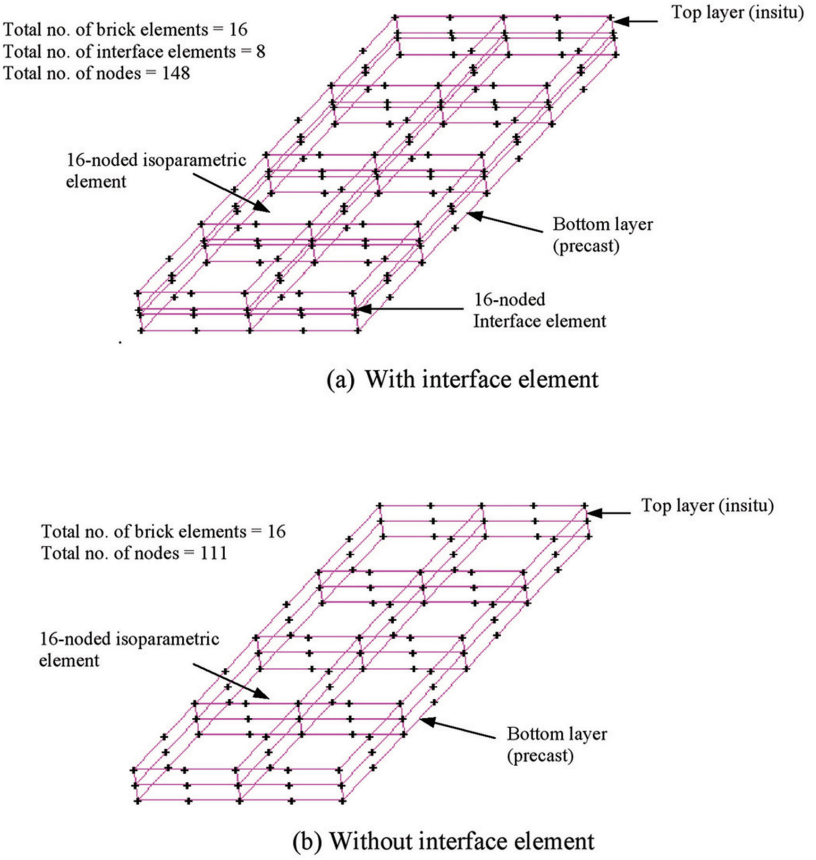

Fig. 4: Finite element mesh of the precast composite slab unit

TABLE 1
The value of normal and shear stiffness

Case No.	Normal Stiffness, K_{nn} (kN/m^2)	Shear Stiffness, K_{ss} (kN/m^2)
I	10e7	10e7
II	10e7	10e5
III	10e7	10e4
IV	10e7	100
V	10e7	50
VI	10e7	10
VII	10e7	0
VIII	without interface	without interface

DISCUSSION OF RESULTS

The structural behaviour of the composite slab has been discussed, with respect to displacements, strains, principal stresses and normal stresses.

Figs. 6 and *7* show the variations of vertical displacement of the precast composite slab along section A-A and B-B (*Fig. 5*), respectively. The variations of displacement for Case III, IV, V, VI, and VII gave almost the same results. It could also be seen from these plots that as the value of K_{ss} had reduced, while the deflections were increasing. Furthermore, the variations of displacement for Case I with high value of shear stiffness (K_{ss} = 10e7) are almost similar to the results where no interface elements (Case VIII) were involved.

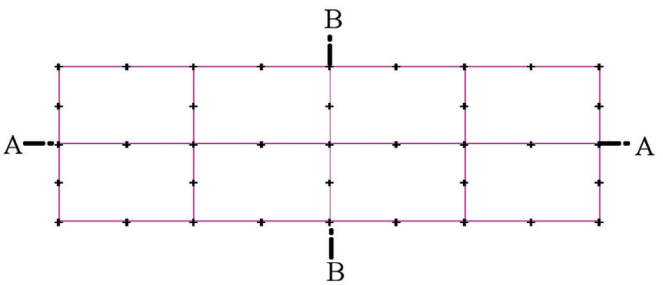

Fig. 5: Section lines for displacement analysis

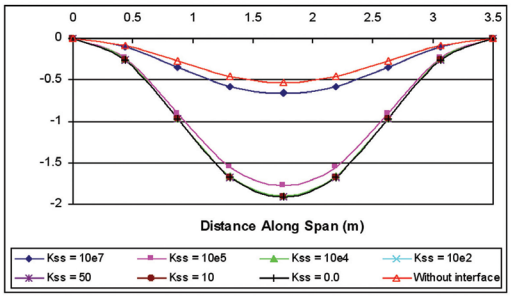

Fig. 6: Vertical displacement (A-A)

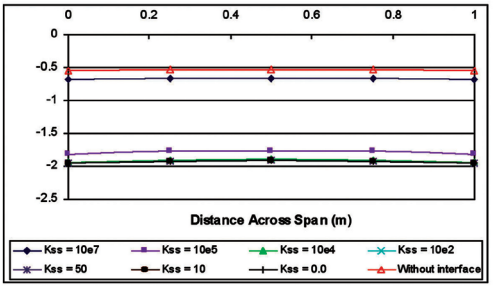

Fig. 7: Vertical displacement (B-B)

Strains

The complete composite action, with respect to strain variation along the depth (thickness) of the slab, is presented in this section. The strains are plotted along the depth of the composite slab at two Gaussian points, namely Point (I) and Point (II), as indicated in *Fig. 8* (i.e. the nearest Gauss point to C-C).

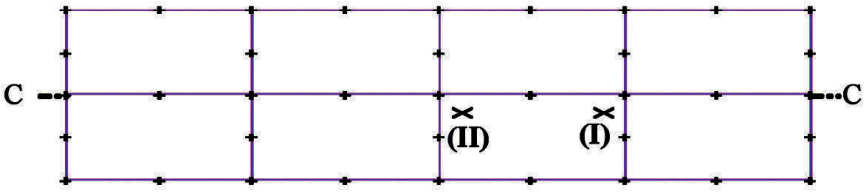

Fig. 8: Location for the strain analysis

The variation of the strain along the depth is shown in *Figs. 9* and *10*. It can be seen that case VIII shows a similar trend of behaviour as i.e. full bond case I when there is no interface, and the slab behaves as one unit. Meanwhile, when there is partial bond or no bond (case II to VII), the plots clearly shows that the two layers behave independently.

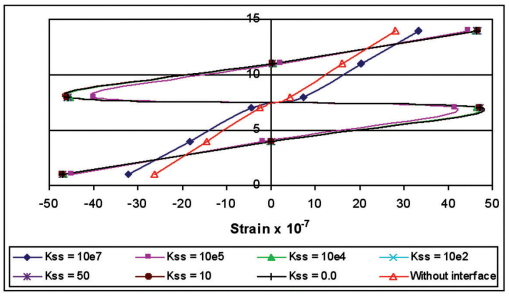

Fig. 9: Strain along depth (Point I)

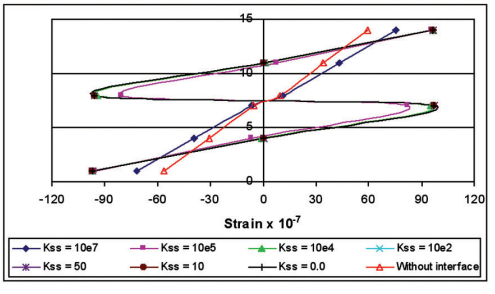

Fig. 10: Strain along depth (Point II)

Stresses

The variations of the maximum principal stresses (σ_1) and the minimum principal stresses (σ_3), to the nearest Gaussian integration point to section D-D and E-E (*Fig. 11*), are shown in *Figs. 12* to *15*. The above stresses were plotted for different layers, the *in situ* (top) and precast (bottom), which were plotted separately.

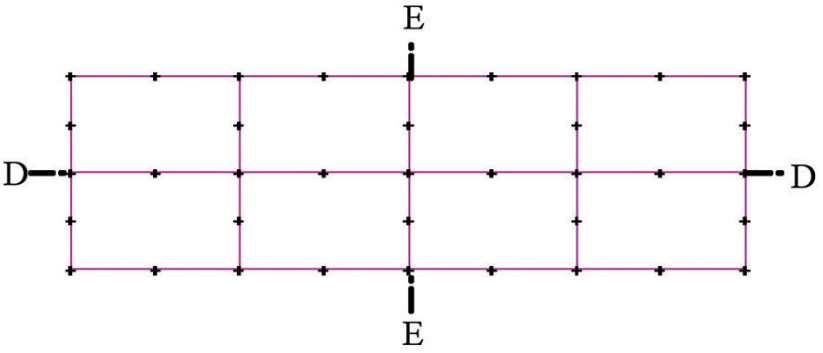

Fig. 11: Section lines for stress analysis

Figs. 12 and *13* show the patterns of the variation for the maximum stresses along section D-D and E-E. It is evident from these plots that Case I and Case VIII have resulted in the same behaviour. Similarly, it is also clear from these plots that both the layers have exactly opposite signs, and in the middle portion, the top layer is in compression while the bottom layer in tension.

The minimum principal stresses σ_3 (kN/m2) were plotted for the similar sections as σ_1 and these are illustrated in *Figs. 14* and *15* below.

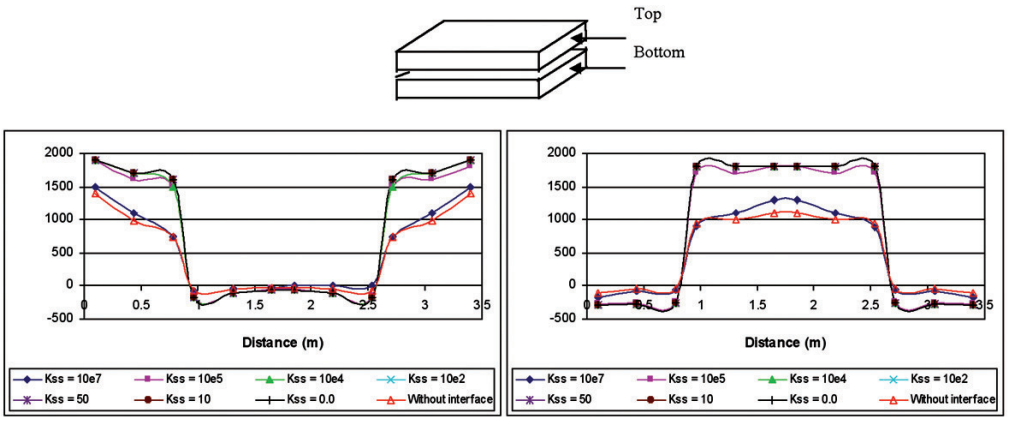

(a) Top Layer (b) Bottom Layer

Fig. 12: Variations of the maximum principal stress, σ_1 along Section D-D

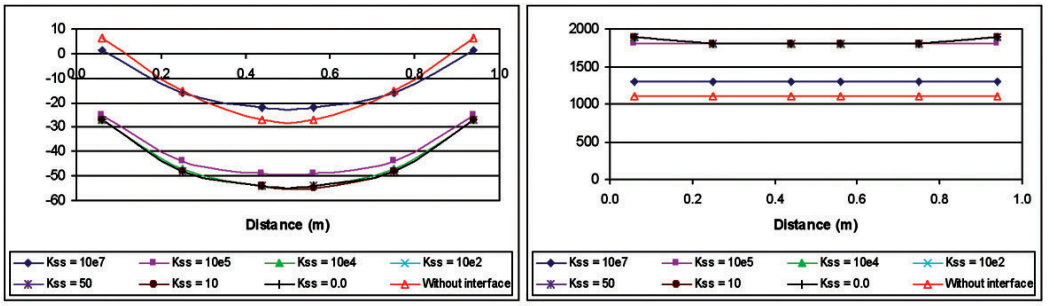

(a) Top Layer (b) Bottom Layer

Fig. 13: Variations of the maximum principal stress, σ_1 along Section E-E

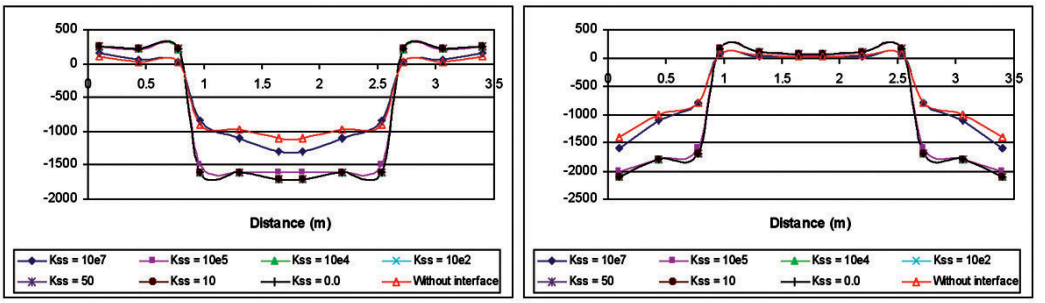

(a) Top Layer (b) Bottom Layer

Fig. 14: Variations of the minimum principal stress, σ_3 along Section D-D

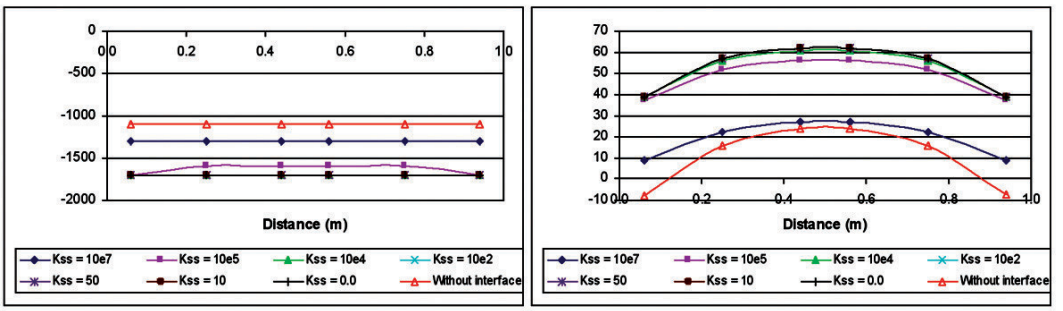

(a) Top Layer (b) Bottom Layer

Fig. 15: Variations of the minimum principal stress, σ_3 along Section E-E

THE STUDY OF THE NORMAL AND SHEAR STRESSES AT CONTACT SURFACE

In the formulation of the interface element, it was seen that there were one normal stress σ_n and two shear stresses τ_{n1} and τ_{n2}. In this study, the variation of the normal stress σ_n, along Section N-N and O-O (*Fig. 16*), are as shown in *Figs. 17* and *18*. These plots indicate that there is no separation between the layers and the complete contact is due to their nature of the loadings.

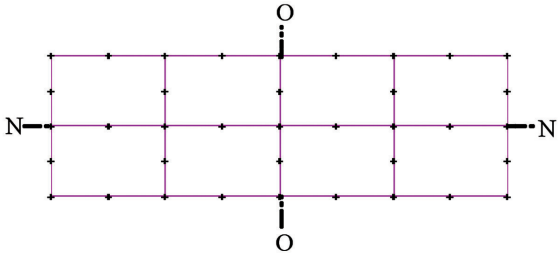

Fig: 16: Section lines for the interface element analysis

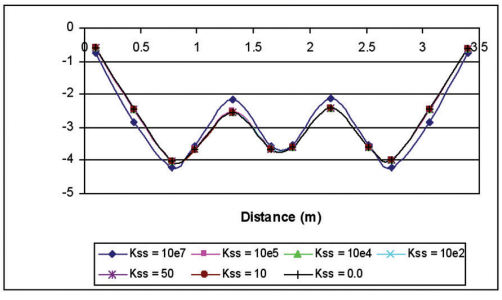

Fig. 17: Normal Stress, σ_n (N-N)

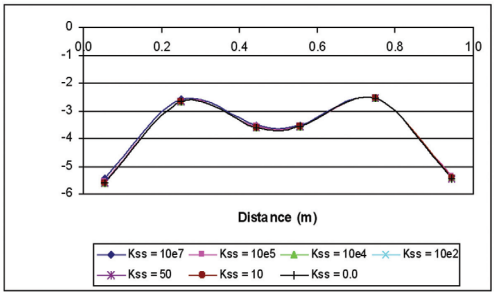

Fig. 18: Normal Stress, σ_n (O-O)

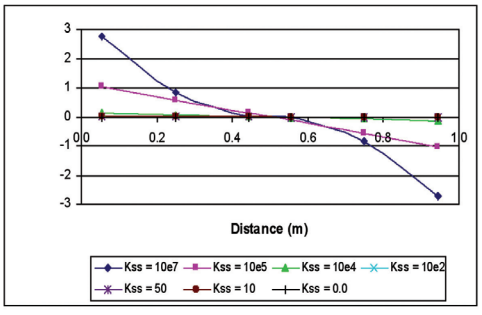

Fig. 19: Shear Stress, τ_{n1} (N-N)

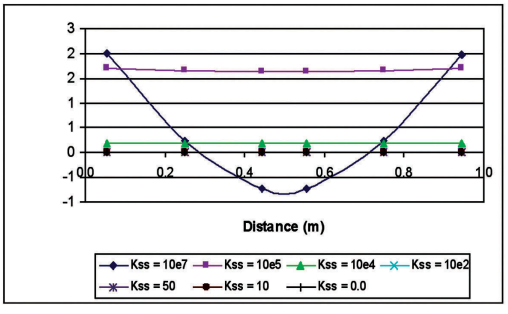

Fig. 20: Shear Stress, τ_{n1} (O-O)

Figs. 19 and *20* show the variations of the shear stress, τ_{n1} i.e. the shear stress in *x*-direction. From these plots, it is clear that the shear stress reduces when the value of shear stiffness is lower. As for the case where K_{ss} = 10 and K_{ss} = 0.0, the value of τ_{n1} is almost equal to zero and for the high value of K_{ss}, the linear variation follows the same path as that of the shear force

Figs. 21 and *22* below illustrate the variations of τ_{n2} (shear stress in z-direction), along the length of the slab (Section E-E) and across the slab (Section F-F). It can be stated that the resistance of the slab in the two-directions is according to the values of shear stiffness K_{ss}.

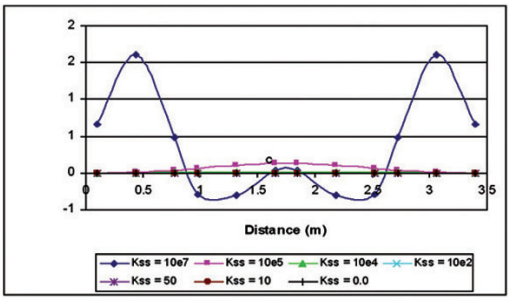

Fig. 21: Shear Stress, τ_{n2} (N-N)

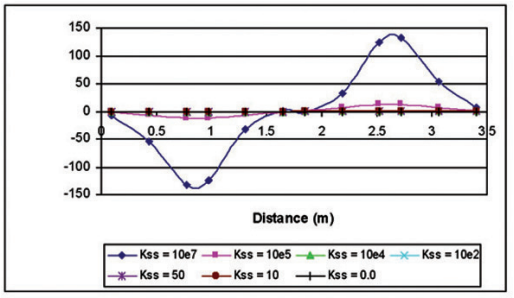

Fig. 22: Shear Stress, τ_{n2} (O-O)

CONCLUSIONS

In the case of the composite slab, the slab consists of two layers which are constructed at different stages (the precast layer in industry and the other layer cast at the construction site). In this situation, it is necessary to model the interfacial behaviour between the two layers, using the interface element. Therefore, this study has given a special attention to this particular type of slab by considering each layer separately and connecting them mathematically through the interface element. Based on the findings, it is revealed that the slab acts as a single unit in the case of full bond.

REFERENCES

Baskar, K. and Shanmugam, N.E. (2003). Steel-concrete composite plate girders subject to combined shear and bending. *Journal of Constructional Steel Research, 59*(4), 531-557.

Hanson, J.H., Bittencourt, T.N. and Ingraffea, A.R. (2004). Three-dimensional influence co-efficient method for cohesive crack simulations. *Engineering Fracture Mechanics, 71*(15), 2109-2124.

Mishuris, G. and Öchsner, A. (2005). Edge effects connected with thin interphases in composite materials. *Composite Structures*, *68*(4), 409-417.

Nassif, H.H. and Najm, H. (2004). Experimental and analytical investigation of ferrocement-concrete composite beams. *Cement & Concrete Composites*, *26*(7), 787-796.

Noorzaei, J., Jaafar, M.S., Thanoon, W.A. and Ghafouri, H.R. (2003). Software development for the analysis of arch dams under static and dynamic loads. *IEM Journal*, *64*(2), 31-39.

Pande, G.N. and Sharma, K.G. (1979). On joint/interface element and associated problems of numerical ill-conditioning. *International Journal Analysis and Numerical Method in Geomechanics*, *2*(3), 293-300.

Tzamtzis, A.D. and Asteris, P.G. (2004). FE analysis of complex discontinuous and jointed structural systems (Part 1: Presentation of the method – A state-of-the-art review). *Electronic Journal of Structural Engineering*, *4,* 75-92.

Tzamtzis, A.D. and Asteris, P.G. (2004). FE analysis of complex discontinuous and jointed structural systems (Part 2: Application of the method-development of a 3D model for the analysis of unreinforced masonry walls). *Electronic Journal of Structural Engineering*, *4,* 93-107.

Viladkar, Noorzaei, J. and Godbole, P.N. (1994). Modelling of interface for soil structure interaction studies. *International Journal of Computer and Structures, Pergamon, United Kingdom*, *52*(4), 765-779.